Short communication

Silicon-coated carbon nanofiber hierarchical nanostructures for improved lithium-ion battery anodes

Gerard K. Simon [a,d,*], Benji Maruyama [b], Michael F. Durstock [b], David J. Burton [c], Tarun Goswami [d]

[a] Air Force Research Laboratory, Materials and Manufacturing Directorate, AFRL/RXBC, 2941 Hobson Way, Wright Patterson AFB, OH 45433-7750, USA
[b] Air Force Research Laboratory, Materials and Manufacturing Directorate, AFRL/RXBN, 2941 Hobson Way, Wright Patterson AFB, OH 45433-7750, USA
[c] Applied Sciences, Inc., 141 West Xenia Avenue, Cedarville, OH 45014-0579, USA
[d] Biomedical, Industrial and Human Factors Engineering, Wright State University, 207 Russ Engineering Center, Dayton, OH 45435, USA

ABSTRACT

Silicon-coated carbon nanofibers (CNFs) are a viable method of exploiting silicon's capacity in a battery anode while ameliorating the complications of silicon expansion as it alloys with lithium. Silicon-coated CNFs were fabricated through chemical vapor deposition and deposited onto a carbon fiber mesh. This novel anode material demonstrated a capacity of 954 mAh g^{-1} in the first cycle, but faded to 766 mAh g^{-1} after 20 cycles. Structural characterization of the samples before and after cycling was carried out using field-emission scanning electron microscopy (FESEM) and transmission electron microscopy (TEM). The results suggest that a portion of the fade may be due to separation of the silicon coating from the CNFs. Enough silicon remains in contact with the conductive network of CNFs to allow a usable reversible capacity that well exceeds that of graphite. An anode of this material can double the capacity of a lithium-ion battery or allow a 14% weight reduction.

Published by Elsevier B.V.

1. Introduction

The demand for high capacity lithium-ion batteries is increasing with numerous portable devices coming to the market. Additionally, high capacity batteries are being sought for applications such as electric automobiles and implantable medical devices. Graphite is currently the anode material of choice for commercial lithium-ion batteries. It intercalates lithium well, with a theoretical specific capacity of 372 mAh g^{-1}, is inexpensive, and widely available. Its limit on the specific capacity is partially imposed by the thermodynamic equilibrium saturation composition of LiC$_6$ [1,2]. In practice, one can expect to attain a reversible capacity in the vicinity of 350 mAh g^{-1} [1–3]. Increasing the capacity may be accomplished by the incorporation of elements with a much greater capability to bind with lithium than graphite. Silicon, tin, and tin oxide (SnO$_2$), for example, are materials that have a much higher theoretical capacity than graphite. Silicon's theoretical capacity is 4200 mAh g^{-1} [4], while tin and tin oxide have theoretical capacities of 981 and 1491 mAh g^{-1}, respectively [5]. However, they undergo large volume changes when they alloy with lithium [6]. This amount of expansion and con-

traction causes pulverization of bulk or thin film anodes [4], which degraded the electrical continuity within the electrode. This requires new strategies for using tin and silicon in battery anodes.

Nanocomposites of silicon and carbon as well as nanowires have been studied for capturing the benefits of silicon while mitigating the effects of its expansion when alloying with lithium. In nanocomposites, the carbon component is intended to serve a dual function, facilitating electron transport to the silicon nanoparticles, while at the same time accommodating silicon volume changes. Some nanocomposites have been fabricated with pyrolyzed, mechanically milled silicon and polystyrene resin [7] or by moderate ball milling of carbon (graphite, disordered carbon, meso carbon microbeads, etc.) and nanocrystalline Si [8,9]. They have produced reversible capacities from 800 to 1400 mAh g^{-1}. In nanocomposites, long ball-milling times, exceeding 5 h, may lead to the formation of silicon-carbide (SiC) [10,11], which is electrochemically inactive and does not contribute to the capacity of the anode [7,12]. This often leads to the use of buffer materials in the milling operation that allow extended milling times and produces materials with reversible capacities of 660–640 mAh g^{-1}, at 160 mA g^{-1} [13]. There is almost no capacity fade after 25–30 cycles with these materials. A hierarchical nanocomposite fabricated from ball-milled carbon nanotubes (CNTs), carbon nanofibers (CNFs), and silicon with carboxymethyl cellulose as a binder, produced very good results [14]. Its reversible capacity at 125 cycles at C/6 was a commendable 800 mAh g^{-1}. In this material, the CNFs boost the

---

* Corresponding author at: Air Force Research Laboratory, Materials and Manufacturing Directorate, AFRL/RXBC, 2941 Hobson Way, Wright Patterson AFB, OH 45433-7750, USA. Tel.: +1 937 255 1471; fax: +1 937 656 4706.
E-mail address: gerard.simon@wpafb.af.mil (G.K. Simon).

electrochemical performance by improving electrical conductivity within the anode and connecting the silicon grains.

Nanowires allow silicon to undergo facile strain relaxation, expanding freely radially and axially, consistent with prior work which indicated that particles small in size (micro or nanoscale) will not fracture any further [4,15,16]. Silicon nanowires grown on stainless steel by the vapor–liquid–solid template free growth method [16–19] have demonstrated a reversible capacity of 3193 mAh g^{-1} over 10 cycles [4].

While the previously discussed studies have produced commendable results, it is prudent to continue to explore other methods to incorporate silicon into anodes. This study explores the utility of a silicon-coated hierarchical material and its ability to mitigate the challenges posed by silicon. The material, called Nanomat (Applied Sciences Incorporated (ASI), Cedarville, OH), was used for this study.

Nanomat consists of CNFs that range from 60 to 150 nm in diameter and from 50 to 100 μm in length. These CNFs are scattered throughout a network of carbon fibers (CFs), which provide both an electrical conduction system and a support mechanism for the material. The entire system is coated with a layer of silicon by a proprietary process (Fig. 1).

2. Experimental

The silicon coated Nanomat material was cut into 5 mm × 5 mm sections from 4 cm × 4 cm sheets for electrochemical testing. No further processing was required.

Electrochemical testing was performed in an argon-filled glove box (MBraun). The cut sections were mounted onto copper electrodes and covered with a Celgard 2500 membrane soaked in electrolyte and a lithium foil disk (Aldrich). A second copper electrode placed on top completed the circuit and the entire assembly was held together with a Swagelok fitting. The electrolyte used was 1 M LiBF$_4$ in a 1:1 mixture of diethylene carbonate and ethylene carbonate. The half-cells were cycled 20 times from 0.02 V to 2 V at a 50 mA g^{-1} rate with a Maccor 4300 battery testing system. The coated Nanomat was also tested on a multiple-rate program that ran the samples at 25 mA g^{-1}, 50 mA g^{-1}, 100 mA g^{-1}, 250 mA g^{-1}, 250 mA g^{-1}, 500 mA g^{-1}, and 1000 mA g^{-1}. Prior to electrochemical testing, the samples were heated on a hot plate in the glove box for 1 h at 250 °C, ensuring that any surface moisture was removed. Also, to better understand the contributions of the silicon and the CF/CNF substructure to the electrochemical performance, uncoated Nanomat samples were also run through a multiple-rate program.

Transmission electron microscope (TEM) and field-emission scanning electron microscope (FESEM) images of the fibers before and after cycling were captured with a FEI Titan TEM and a FEI Sirion FESEM. In preparation for TEM imaging, the Nanomat was broken apart with a razor and briefly sonicated in acetone. After dispersion, the CNF suspension was drop-cast onto a holey-carbon/copper grid. The TEM accelerating voltage was 200 kV, while the FESEMs was 10 kV.

3. Results and discussion

In the fabrication of Nanomat, uncoated CNFs were deposited onto continuous rolls of non-woven polyacrylonitrile derived CFs held together with a polymeric binder. The uncoated material consists of 50% CF and 50% CNF (PR-24-XT-LHT), determined by weight, with an areal weight of 25 g m^{-2} (0.125 g cm^{-3} density). The majority of the material's electrochemical capacity is derived from the silicon. The sample used in this study had a silicon weight fraction of 0.368 (determined by weight before and after coating), which allows for a maximum theoretical capacity of 1546 mAh g^{-1} for the
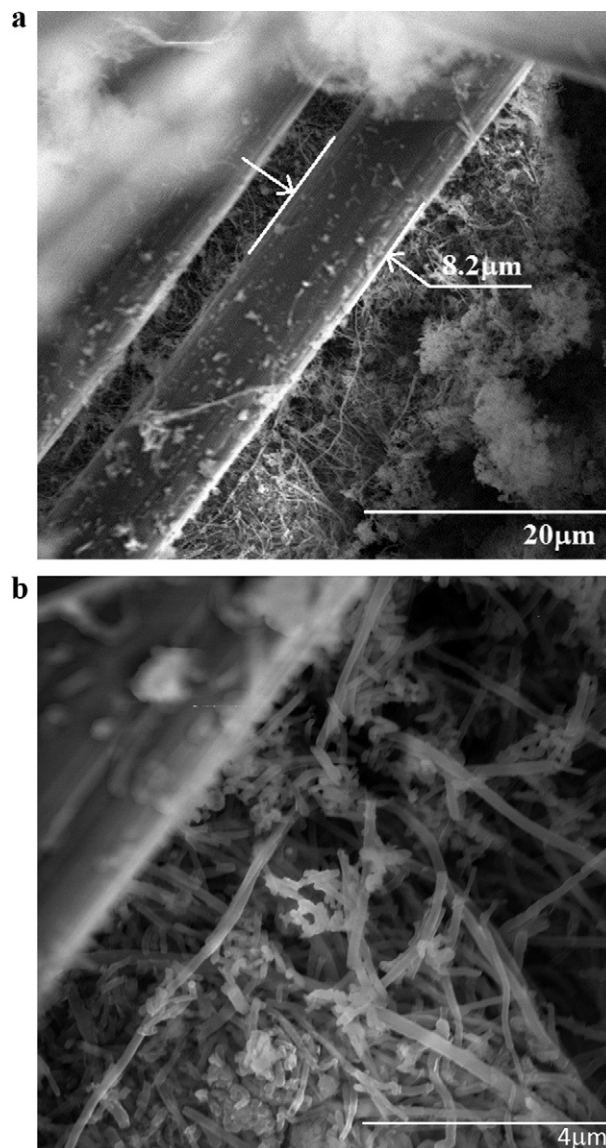

Fig. 1. FESEM images of Nanomat showing the CF structure (top) and the silicon coated CNFs (bottom).

Table 1
Theoretical capacities and contributions of Nanomat constituents.

	Theoretical Capacity	Wt.%	Capacity contribution
Silicon	4200 mAh g^{-1}	36.8%	1546 mAh g^{-1}
Carbon nanofibers	372 mAh g^{-1}	31.6%	118 mAh g^{-1}
Carbon fibers	372 mAh g^{-1}	31.6%	118 mAh g^{-1}
Expected capacity		1782 mAh g^{-1}	

silicon alone (Table 1). With the TEM, the silicon layer is estimated to be 16 nm thick in some locations (Fig. 2), but calculations indicate the silicon thickness may average 19.7 nm throughout the material.

Normally silicon-coated substrates do not function well as lithium-ion battery anodes because the films tend to pulverize and lose electrical contact, leading to capacity fade and shortened battery life [4]. However, the Nanomat material was capable of providing a charge capacity of 786 mAh g^{-1} after 36 cycles at multiple charge/discharge rates when returned to a 50 mA g^{-1} rate, an overall 75% efficiency (Fig. 3). At a fixed 50 mA g^{-1} rate, the reversible capacity after 20 cycles was 766 mAh g^{-1}, an overall 80% efficiency. This performance is comparable to the ball-milled
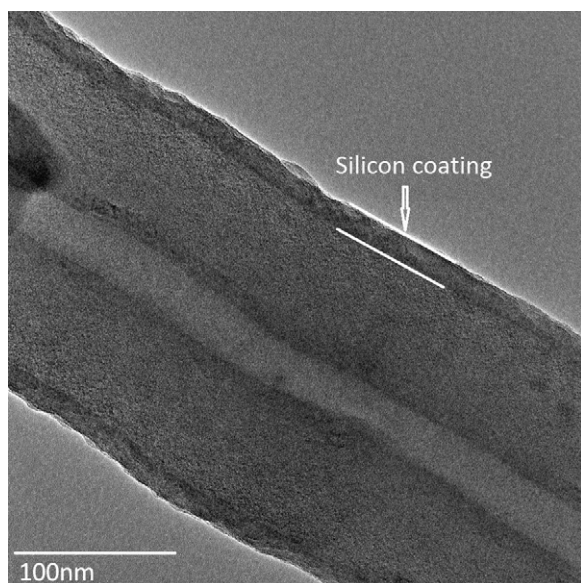
Fig. 2. TEM image of a CNF coated with a 15 nm thick silicon layer.

silicon/carbon nanocomposites, but still inferior to the nanowires. The first cycle discharge and charge capacities at a 25 mA g^{-1} rate were 1787 mAh g^{-1} and 1045 mAh g^{-1}, respectively. We attribute the stability of the material to uniformity of the coating on the CNFs and its resistance to pulverization. The uncoated CF/CNF substructure had a much lower performance. After 36 cycles through an identical test, its reversible capacity was only 62 mAh g^{-1} (Fig. 3). Thus the silicon coating contributes the vast majority of the material's usable capacity.

At a constant 50 mA g^{-1} charge/discharge rate, the Nanomat first cycle discharge capacity was 1956 mAh g^{-1} and the first cycle charge capacity was 954 mAh g^{-1} (Fig. 4). The coated Nanomat showed a long plateau beginning at 0.2 V. This plateau occurs as lithium alloys with silicon to form two phase areas of Si–Li and Si [20]. Successive cycles indicated small but steady drops in the capacity. A portion of the first cycle capacity loss can be attributed to the formation of the SEI layer, but this is difficult to quantify. However, as seen in Fig. 5, there was some separation and tearing of the silicon coating from the underlying support mechanism of CNFs and CFs. This also contributes to capacity losses. Because
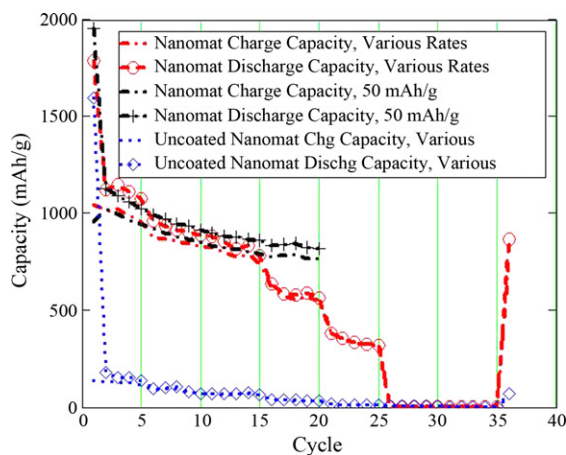

Fig. 3. Charge and discharge capacities of Nanomat at 50 mA g^{-1} rate and various rates: cycles 1–5: 25 mA g^{-1}; cycles 6–15 and 36: 50 mA g^{-1}. Cycles 16–20: 100 mA g^{-1}; cycles 21–25: 250 mA g^{-1}; cycles 26–30: 500 mA g^{-1}; cycles 31–35: 1000 mA g^{-1}.
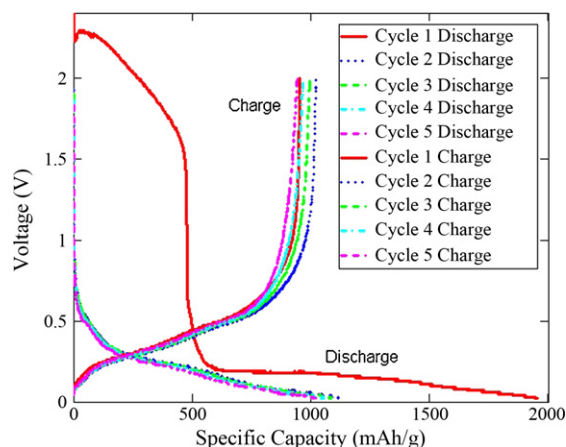

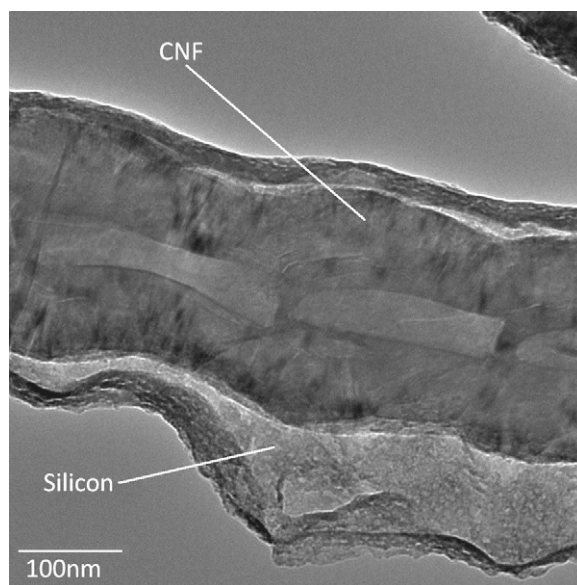**Fig. 4.** Charge and discharge curves of Nanomat at 50 mA g^{-1} rate.

Fig. 5. TEM image of silicon-coated CNF after 20 cycles.

the coating expanded radially, it retained enough electrical contact with the CNFs and CFs to maintain the electrochemical processes, though at a decreased capability. It is also apparent in Fig. 5 that the silicon coating does not return to its original shape upon delithiation. This is consistent with the findings of Yang et al., who observed through models that this is indeed the case with coatings that alloy with lithium [15].

4. Conclusion

Nanomat taps the capacity of silicon through coated CNFs and its unique structure. Prior to cycling, the silicon coating on the CNFs is approximately 19.7 nm thick and very uniform. FESEM and TEM images revealed that despite significant expansion and contraction (the primary source of damage to the coated fibers), the silicon remains in contact with its CNF substrate. Because the silicon coating remains in contact with the CNF, it maintains its ability to deliver high capacity for the anode. With a capacity of 766 mAh g^{-1} after 20 cycles, the performance of this material compares favorably to the mechanically milled and ball-milled nanocomposite anode materials mentioned in Section 1 of this manuscript and is well in excess of graphites capacity.

References

[1] B. Gao, C. Bower, J.D. Lorentzen, L. Fleming, A. Kleinhammes, X.P. Tang, L.E. McNeil, Y. Wu, O. Zhou, Chem. Phys. Lett. 327 (2000) 69–75.
[2] A.P. Legrand, S. Flandrois, Chemical Physics of Intercalation Compounds, 59th ed., Plenum, New York, 1987, pp. 517.
[3] M. Letellier, F. Chevallier, M. Morcrette, Carbon 45 (2007) 1025–1034.
[4] C.K. Chan, H. Peng, G. Lui, K. McIlwrath, X.F. Zhang, R.A. Huggins, Y. Cui, Nat. Nanotechnol. 3 (2008) 31–35.
[5] H. Zhang, C. Feng, Y. Zhai, K. Jiang, Q. Li, S. Fan, Adv. Mater. 21 (2009) 2299–2304.
[6] R.A. Huggins, W.D. Nix, Ionics 6 (2000) 57–63.
[7] I. Kim, P.N. Kumta, J. Power Sources 136 (2004) 145–149.
[8] G.X. Wang, J. Yao, H.K. Liu, Electrochem. Solid State Lett. 7 (2004) A250–A253.
[9] C.S Wang, G.T. Wu, X.B. Zhang, Z.F. Qi, J. Li, J. Electrochem. Soc. 145 (1998) 2751–2758.
[10] M. Sherif El-Eskandarany, K. Sumiyama, K. Suzuki, J. Mater. Res. Soc. 10 (1995) 659–667.
[11] X.Y. Yang, Z.W. Huang, Y.K. Wu, H.Q. Ye, Mater. Sci. Eng. A 300 (2001) 278–283.
[12] M.K. Datta, P.N. Kumta, J. Power Sources 165 (2007) 368–378.
[13] Y.D. Ko, J.G. Kang, J.G. Park, S. Lee, D.W. Kim, Nanotechnology 20 (2009) 455701.
[14] B. Lestriez, S. Desaever, J. Danet, P. Moreau, D. Plee, D. Guyomard, Electrochem. Solid State Lett. 12 (2009) A76–A80.
[15] J. Yang, M. Winter, J.O. Besenhard, Solid State Ionics 90 (1996) 281–287.
[16] K. Lew, L. Pan, E.C. Dickey, J.M. Redwing, Adv. Mater. 15 (2003) 2073–2076.
[17] M.H. Huang, Y. Wu, H. Feick, N. Tran, E. Weber, P. Yang, Adv. Mater. 13 (2001) 113–116.
[18] A.A. Golovin, S.H. Davis, P.W. Voorhees, J. Appl. Phys. 104 (2008) 074301.
[19] S.M. Roper, S.H. Davis, S.A. Norris, A.A. Golovin, P.W. Voorhees, M. Weiss, J. Appl. Phys. 102 (2007) 034304.
[20] U. Kasavajjula, C. Wang, A.J. Appleby, J. Power Sources 163 (2007) 1003–1039.